POLITECNICO DI MILANO

REGION-BASED MAXIMUM LIKELIHOOD RECONSTRUCTION IN POSITRON EMISSION TOMOGRAPHY FOR QUANTITATIVE ONCOLOGICAL ANALYSIS

Elisabetta De Bernardi, Elena Faggiano, Giuseppe Baselli

^{18}F-FDG PET in clinical oncology

^{18}F-FDG uptake in tissues: index of cellular metabolic activity

^{18}F-FDG PET in clinical oncology:

- cancer diagnosis
- cancer staging
- response to therapy assessment

PET is an intrinsically quantitative technique because of:

- radiotracer nature
- attenuation correction

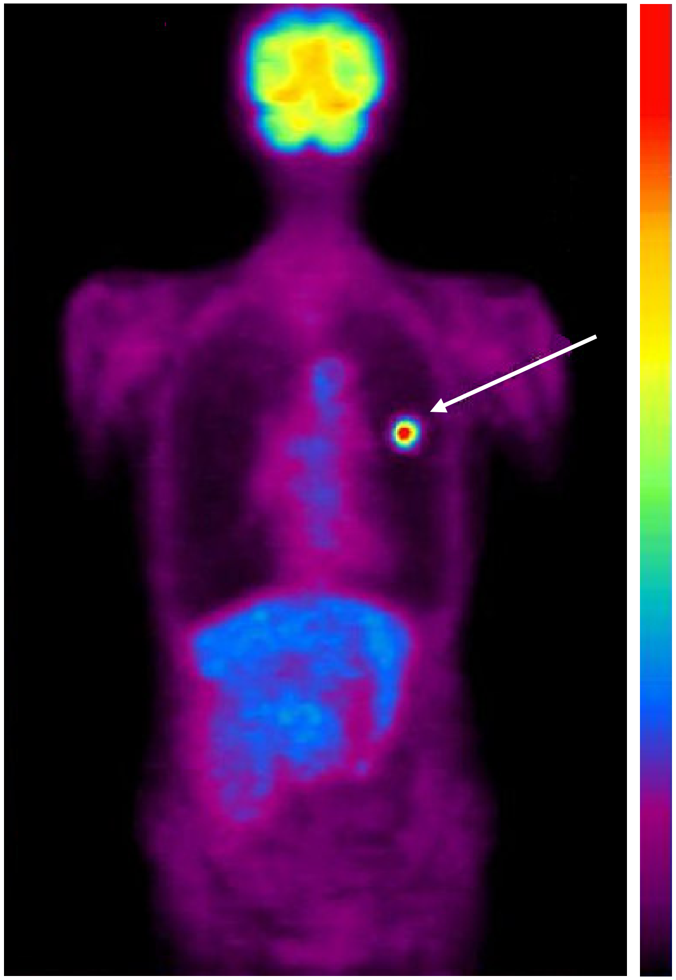

Reconstruction from projections: problem formulation

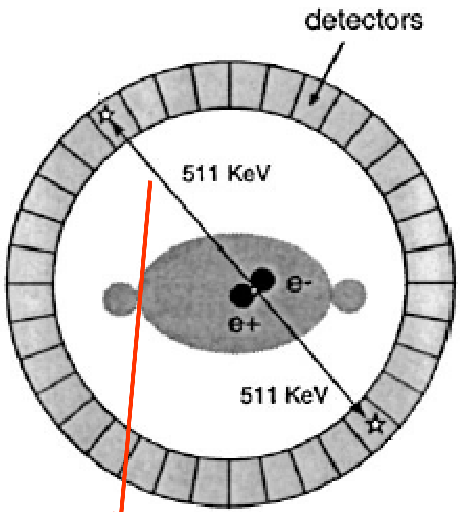

Line Of Response (LOR)

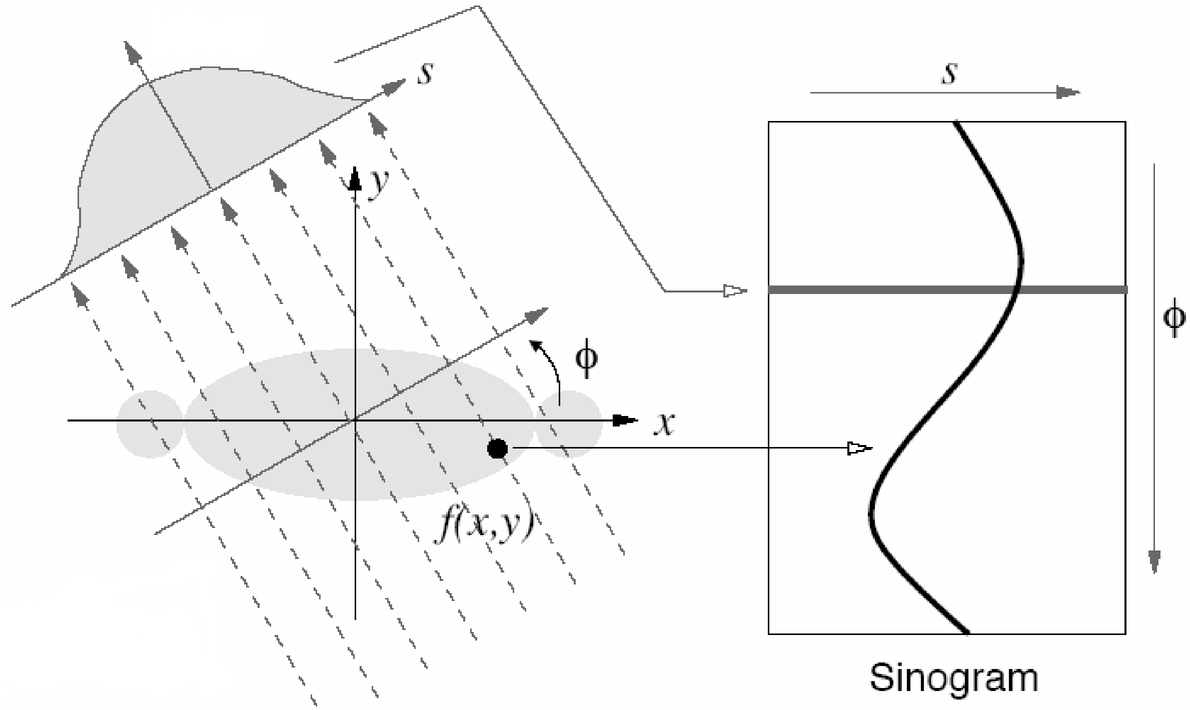

Sinogram

Acquisition process LSV modeling:

$$\overline{Y_i} = E\left[Y_i\right] = \iiint_{FOV} f(x,y,z)\, h_i(x,y,z)\, dxdydz \qquad i = 1,\ldots I$$

Poisson variable

integration kernel

Reconstruction from projections: D-D approach

- Approximation of $f(x,y,z)$ as a linear combination of J basis functions $b_j(x,y,z)$ with unknown weights λ_j:

$$\tilde{f}(x,y,z) = \sum_{j=1}^{J} \lambda_j b_j(x,y,z)$$

- System matrix coefficients computation:

$$a_{ij} = \iiint_{FOV} h_i(x,y,z) b_j(x,y,z)\, dx\, dy\, dz$$

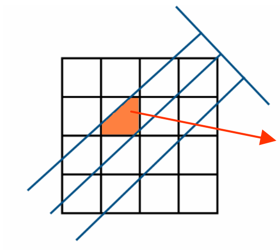

$$\boxed{\overline{Y}_i = \sum_{j=1}^{J} a_{ij} \lambda_j}$$

Reconstruction process: iterative search of λ values optimizing an objective function of the acquired data

Maximum Likelihood iterative reconstruction (MLEM)

- maximization of measured data likelihood function
- expectation maximization algorithm

n^{th} iteration:

$$\lambda_j^{n+1} = \lambda_j^n \cdot \frac{\left(\sum_i a_{ij} \frac{y_i}{\sum_k a_{ik} \lambda_k^n} \right)}{\sum_i a_{ij}}$$

i^{th} LOR error

i^{th} LOR estimated counts

weighted average of the errors

Main factors affecting PET accuracy in clinical practice

- Scanner spatial resolution

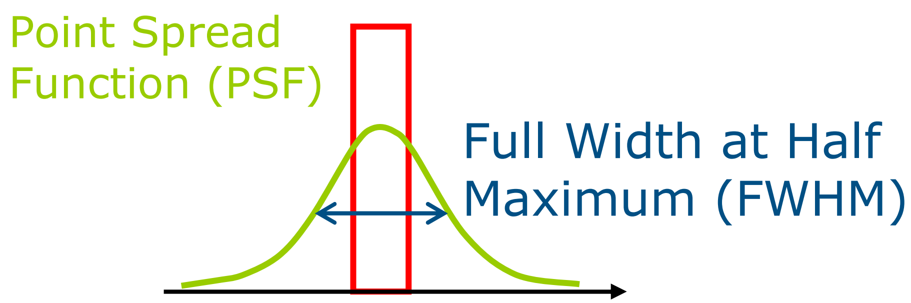

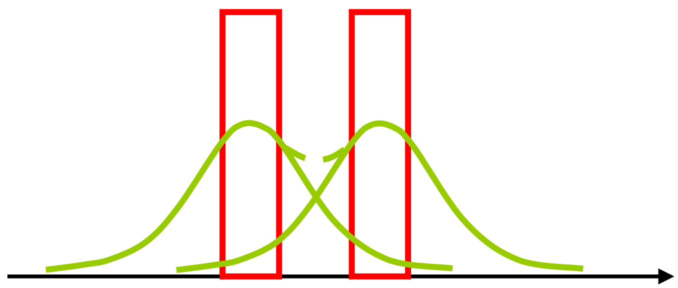

The PSF of a PET scanner is anisotropic and spatially variant (FWHM typically ranges from 4 to 9 mm)

- Noise component

- Reconstruction algorithm characteristics

Scanner PSF modeling and inclusion in MLEM reconstruction

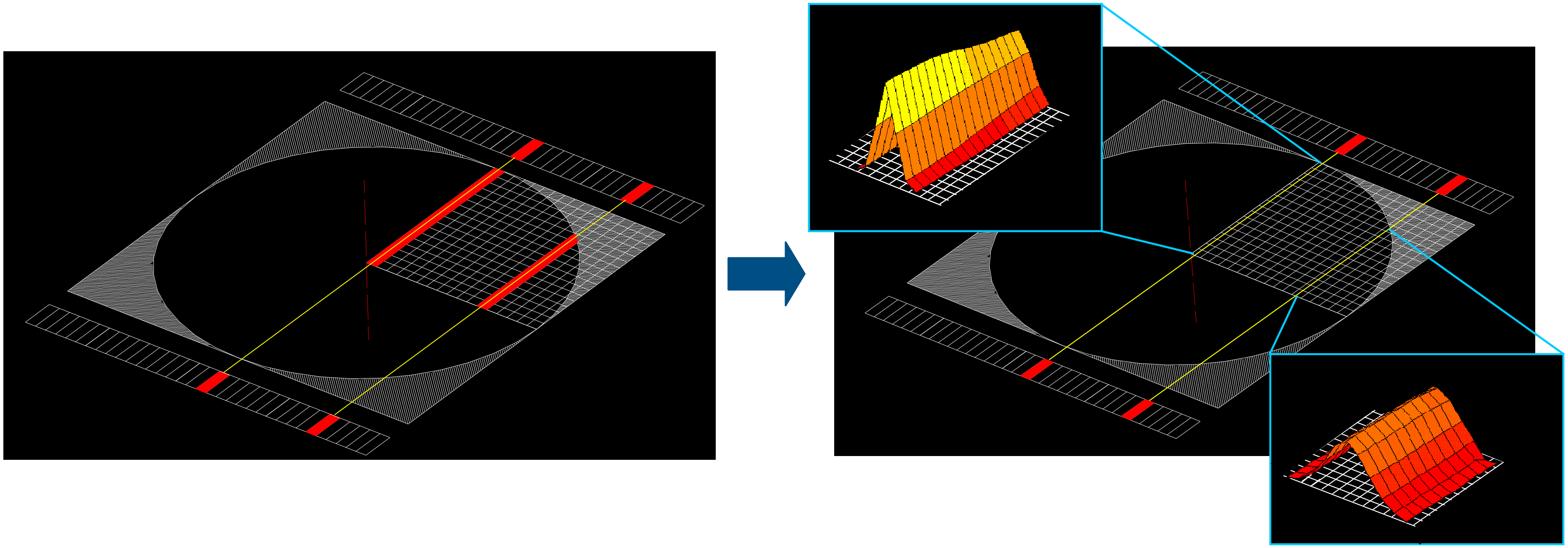

Scanner PSF modeling and inclusion in MLEM reconstruction

Line sources

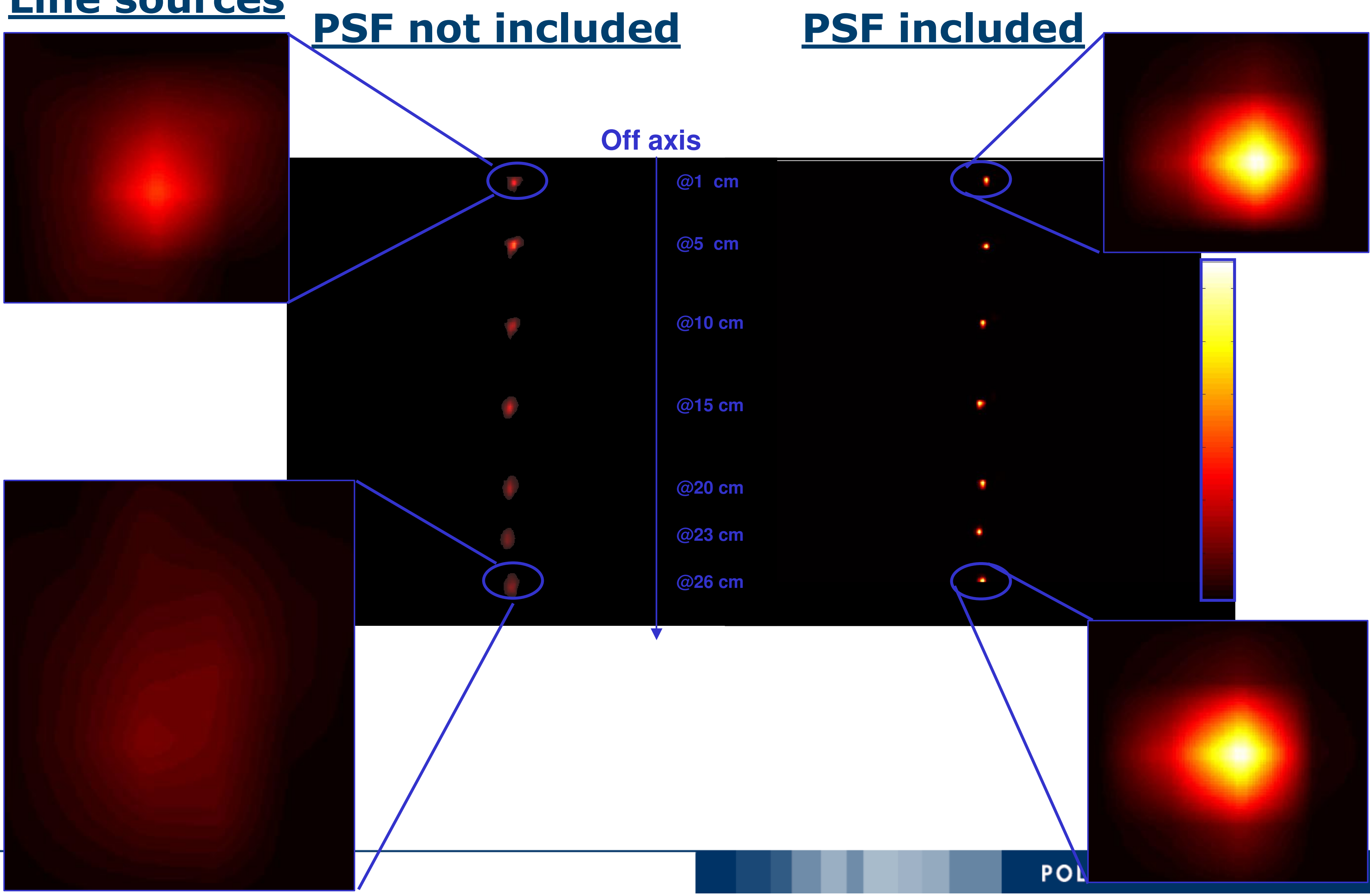

Scanner PSF modeling and inclusion in MLEM reconstruction: <u>results</u>

<u>Maximum likelihood algorithm drawbacks:</u>

- maximum likelihood solution noisy due the problem ill-conditioning: stopping rules and/or post filtering required
- convergence slow and object-dependent

➡ object dependent bias/noise compromise

<u>Effects of PSF inclusion:</u>

- improvement of contrast and quantitative accuracy
- noise component reduction
- Gibbs-like artifacts
- worsening of the object dependent convergence

➡ <u>detectability/quantification trade-off</u>: a more correct quantification of small objects is necessarily associated with larger noise level and larger computation time.

Scanner PSF modeling and inclusion in MLEM reconstruction: results

Lung cancer patient data: 35 mm tumor, large TBR, 3D mode

Without PSF

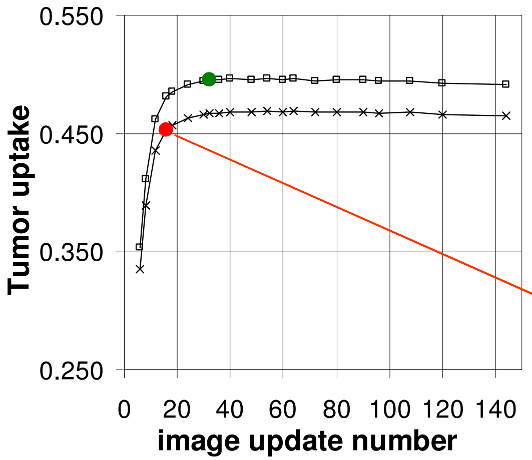

Clinical noise level

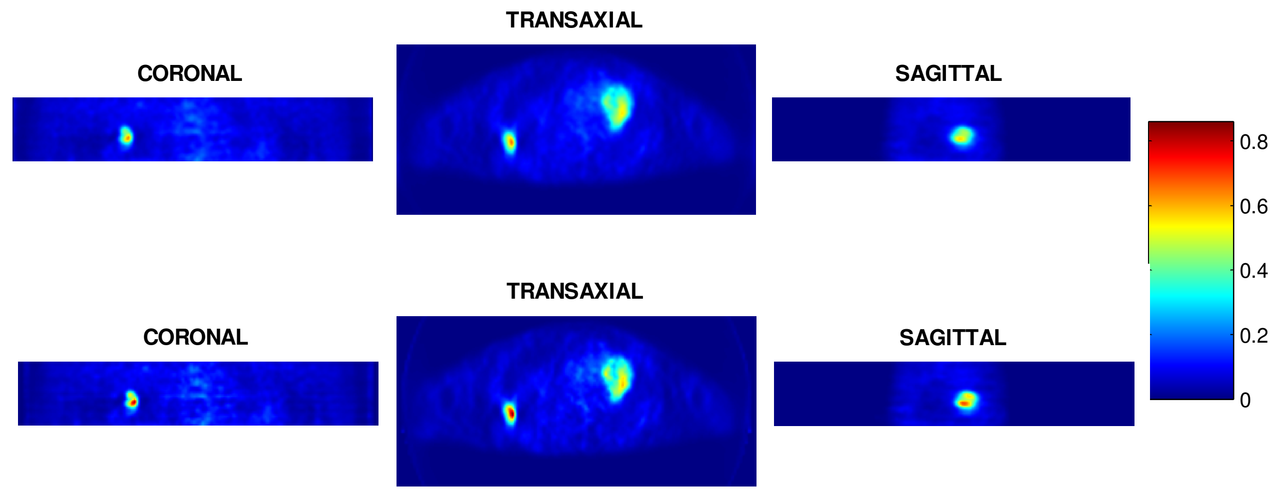

With PSF

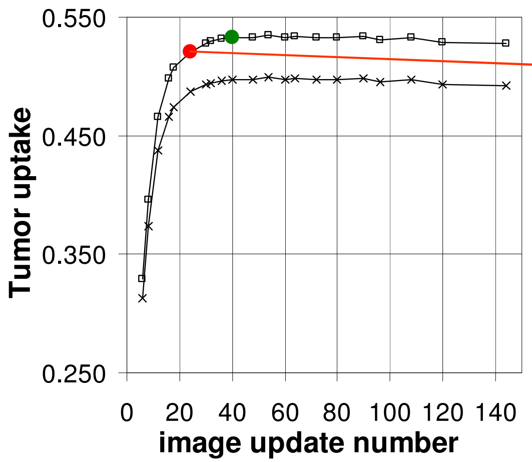

Uptake +28%

Metabolic volume -39%

Scanner PSF modeling and inclusion in MLEM reconstruction: results

Lung cancer patient data: 15 mm tumor, low TBR, 2D mode

Without PSF

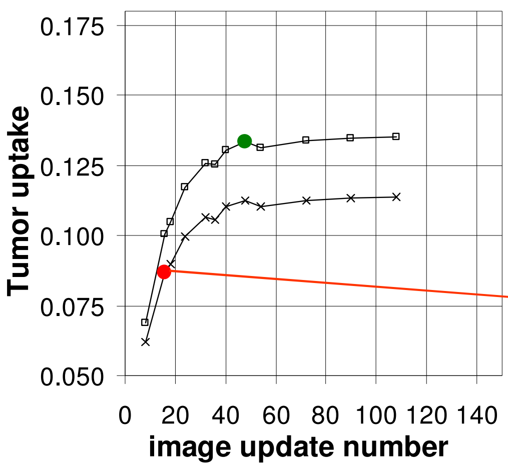

With PSF

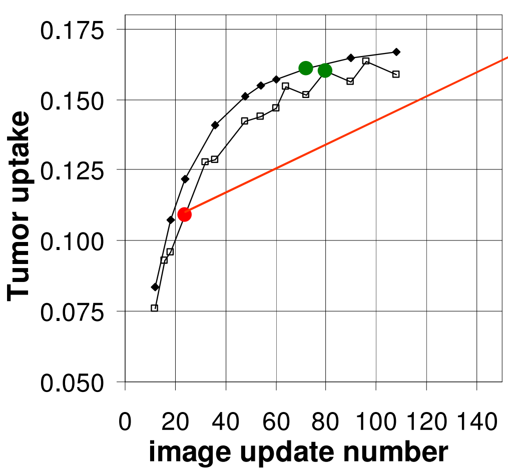

Clinical noise level

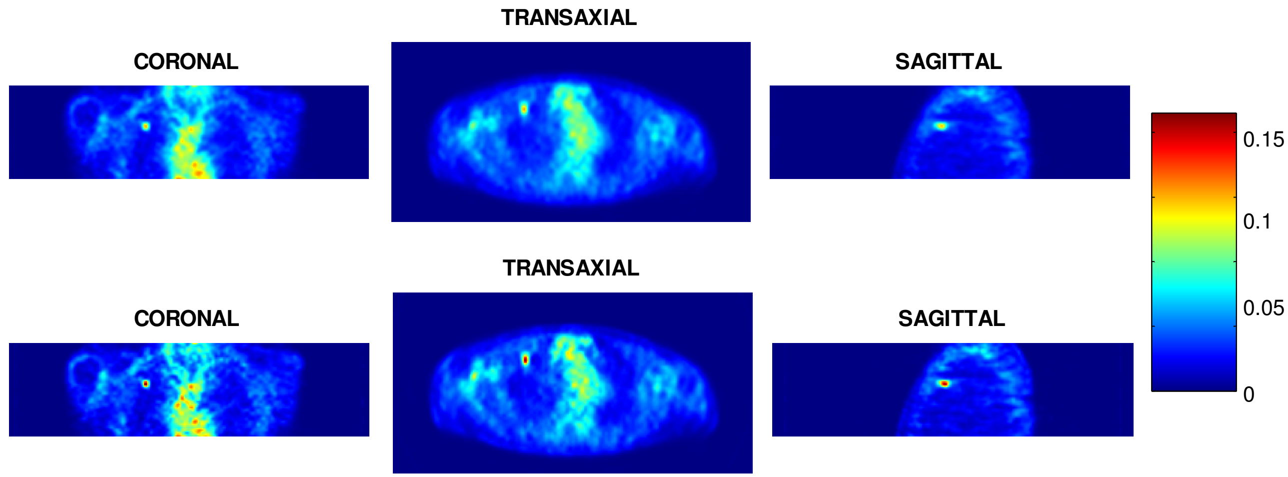

Uptake +39%

Metabolic volume -33%

Region-based MLEM with PSF inclusion for lesion quantification: <u>the idea</u>

- <u>Local quantification tool based on a standard smooth clinical image (STD-CI)</u>

- <u>Definition of regional basis functions on STD-CI</u>:

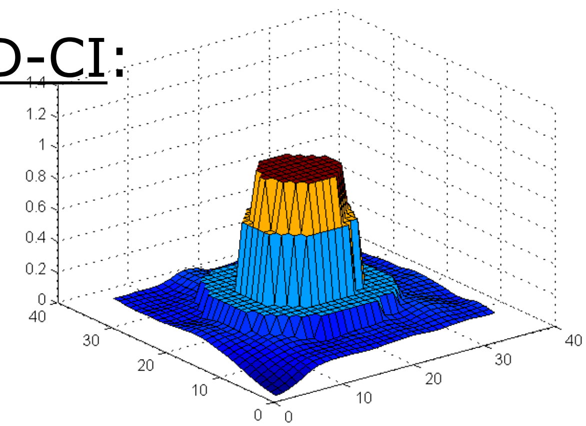

  - the lesion of interest is properly segmented into regional basis functions

  - the image outside the area to be quantified is “frozen” and therefore handled as an unique basis function.

- <u>The ML convergence can be locally achieved without noise increasing</u> (reduced unknown variables; a priori information)

Region-based MLEM: analytical formulation

- STD-CI obtained with a standard voxel-based reconstruction process:

$$I^{STD-CI}(x,y,z)=\sum_{j=1}^{J}\lambda_j^{STD-CI}b_j(x,y,z)$$

- Approximation of *f(x,y,z)* as linear combination of *R* regional basis functions $\beta_r(x,y,z)$ with unknown weights μ_r:

$$\tilde{f}(x,y,z)=\sum_{r=1}^{R}\mu_r\beta_r(x,y,z)$$

- Basis functions definition:

lesion of interest

$$\beta_r(x,y,z)=\begin{cases} T_r(x,y,z)E_{T_r}\left[I^{STD-CI}(x,y,z)\right] & r=1..N \\ T_r(x,y,z)I^{STD-CI}(x,y,z) & r=bkg \end{cases}$$

Region-based MLEM: analytical formulation

- Model of the data collection process:

$$\overline{Y}_i = \sum_{j=1}^{J} a_{ij}\lambda_j = \sum_{r=1}^{R} \tilde{a}_{ir}\mu_r$$

- System matrix coefficients of the region-based problem:

$$\tilde{a}_{ir} = \sum_{j \in T_r} a_{ij}\overline{\lambda}_j$$

with $\overline{\lambda}_j$ = value assumed by the basis function $\beta_r(x,y,z)$ in the j^{th} voxel.

$$\boxed{\mu_r^{n+1} = \mu_r^n \cdot \frac{\left(\sum_i \tilde{a}_{ir} \frac{y_i}{\sum_k \tilde{a}_{ik}\mu_k^n}\right)}{\sum_i \tilde{a}_{ir}}}$$

n^{th} iteration of region-based MLEM reconstruction

Region-based MLEM: preliminary evaluations

Choice of the number of regional basis functions for "uniform" lesions:

- R1: internal region;
- R2: transition region; activity underestimated for partial volume effect;
- R3: external region; activity overestimated for spillout effect

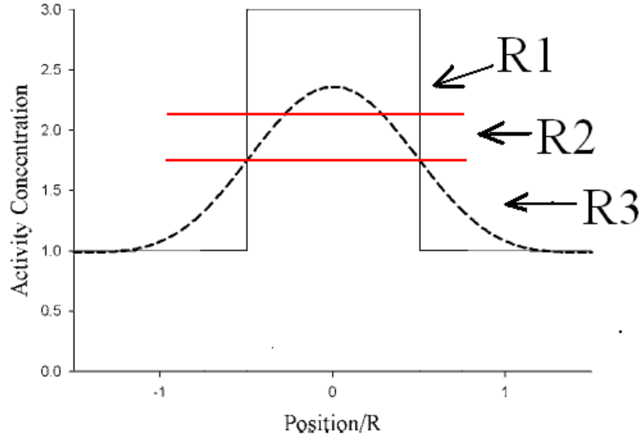

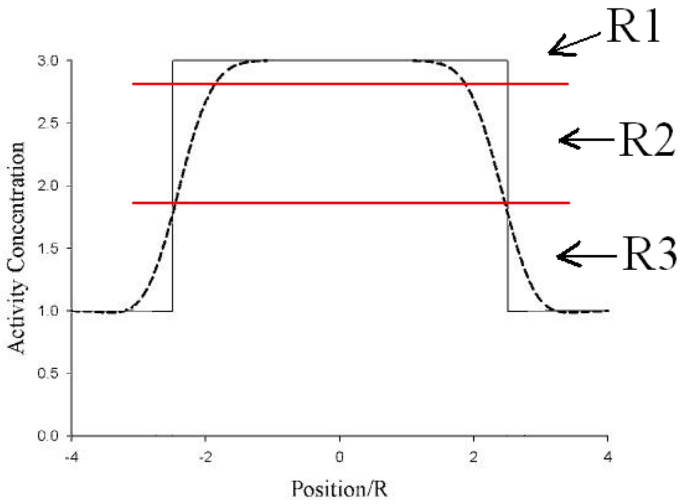

Region-based MLEM: preliminary evaluations

Experimentally acquired sphere phantom

20 iterations

D=9.5mm
TBR=7.5

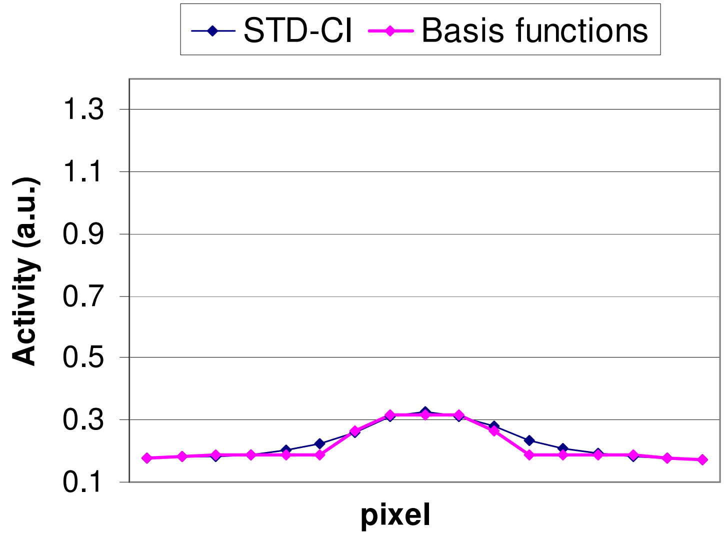

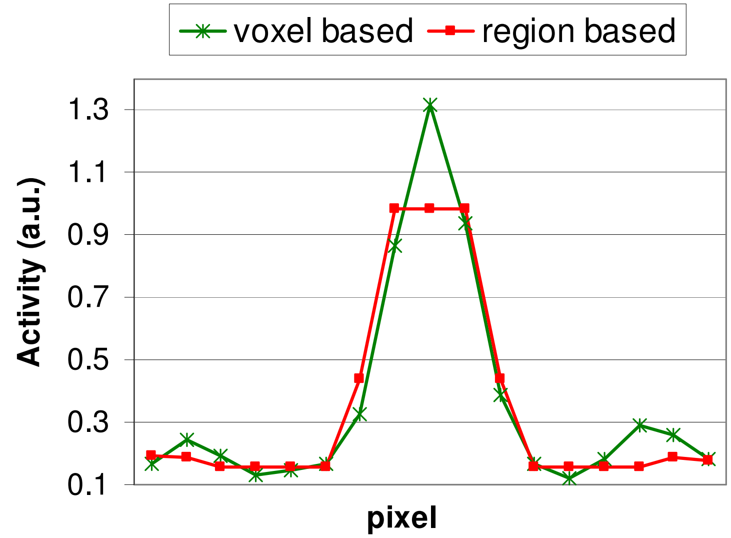

D=28mm
TBR=7.5

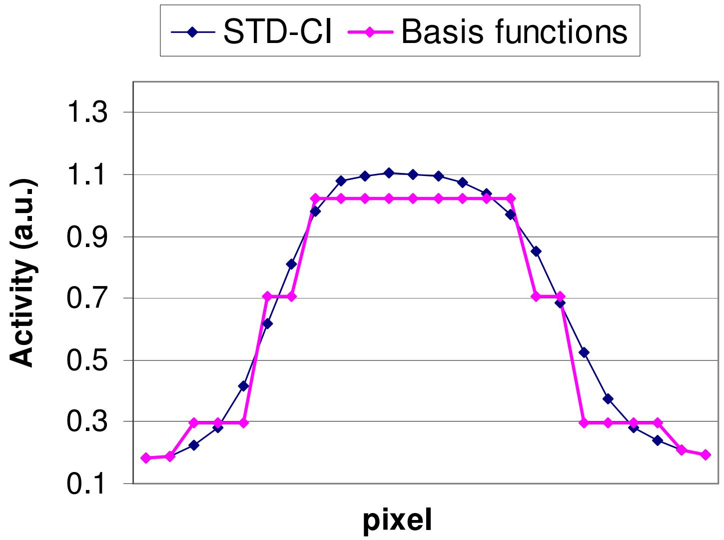

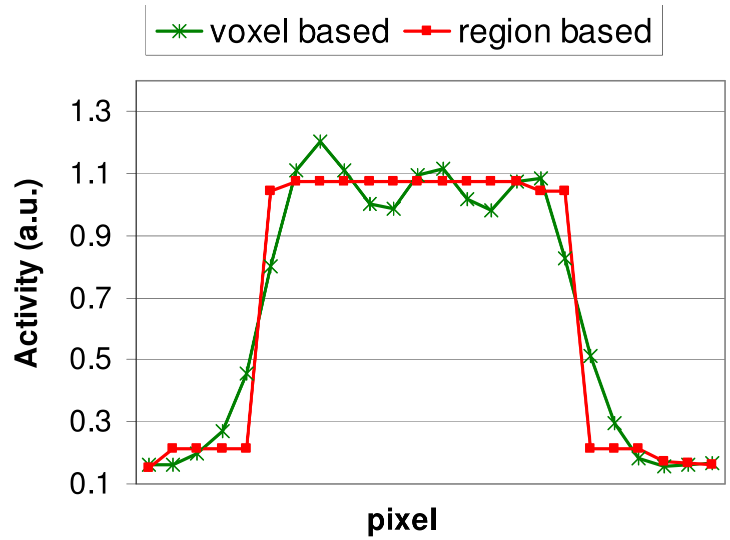

The algorithm

STD-CI

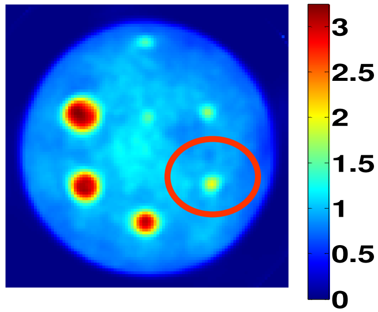

Initial lesion segmentation → Volume Of Interest (VOI) identification → VOI segmentation ($T_r(x,y,z)$) → Regional basis functions ($\beta_r(x,y,z)$) → MLEM reconstruction

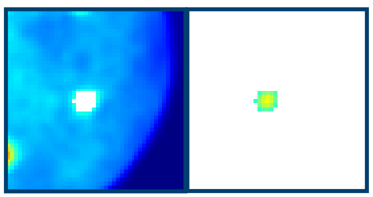

isotropic dilatation of segmented lesion by PSF max (spillout)

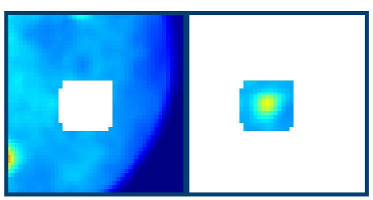

k-means

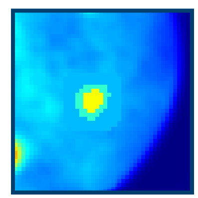

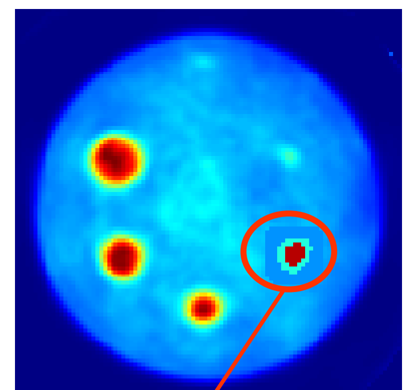

- volume estimate
- FDG uptake estimate

Experimentally scanned sphere phantom: results

Activity contrast=7.5

STD-CI voxel-based region-based

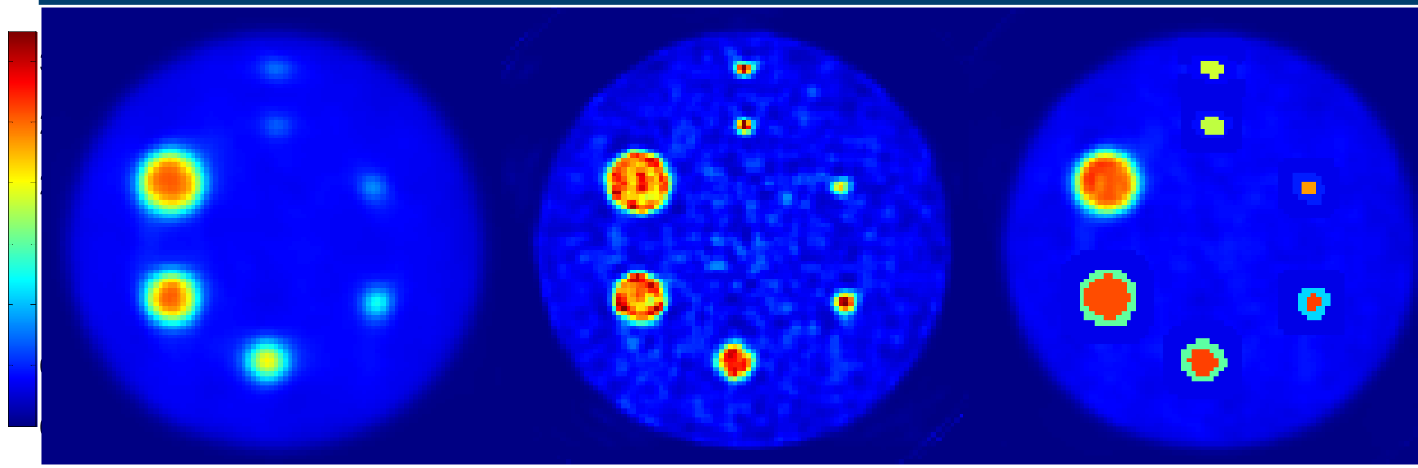

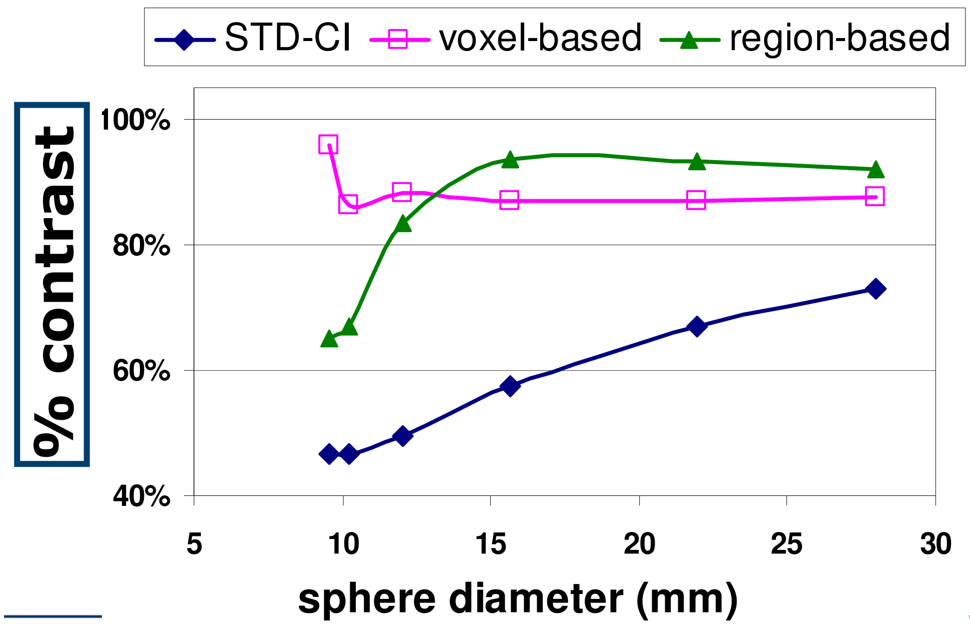

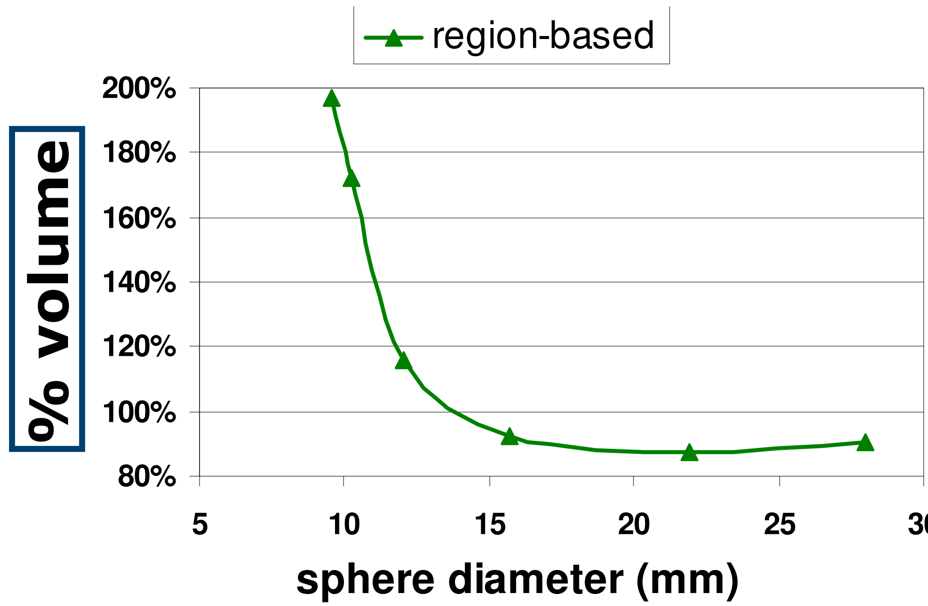

Experimentally scanned sphere phantom: results

Activity contrast=4

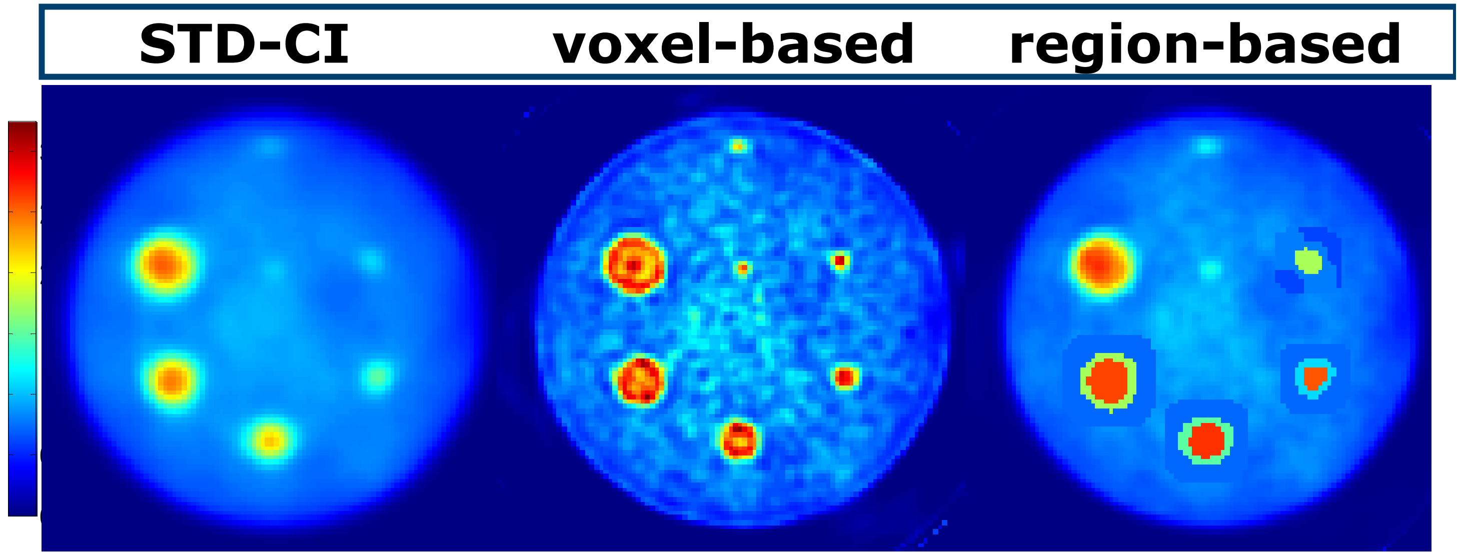

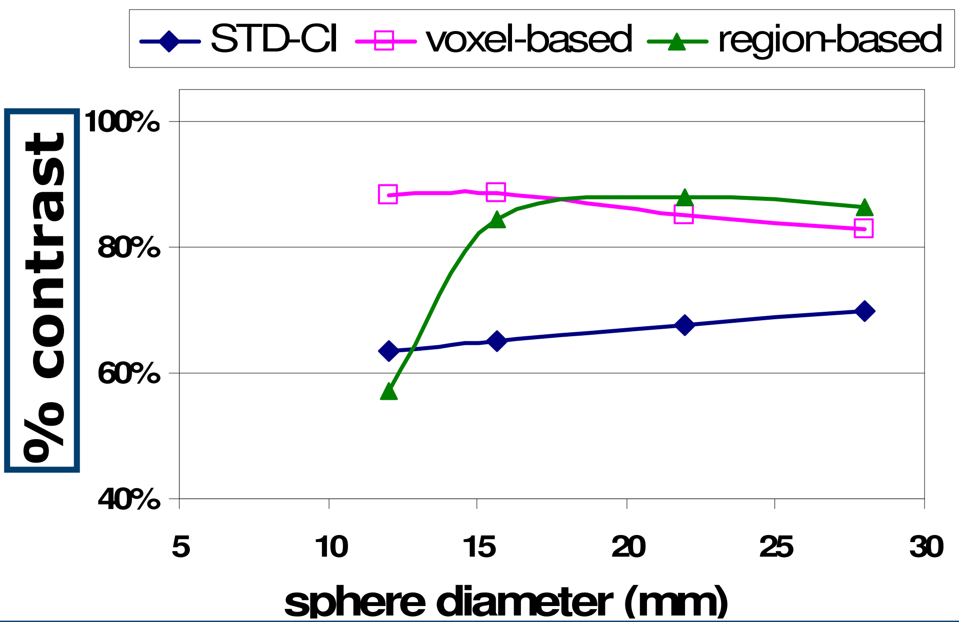

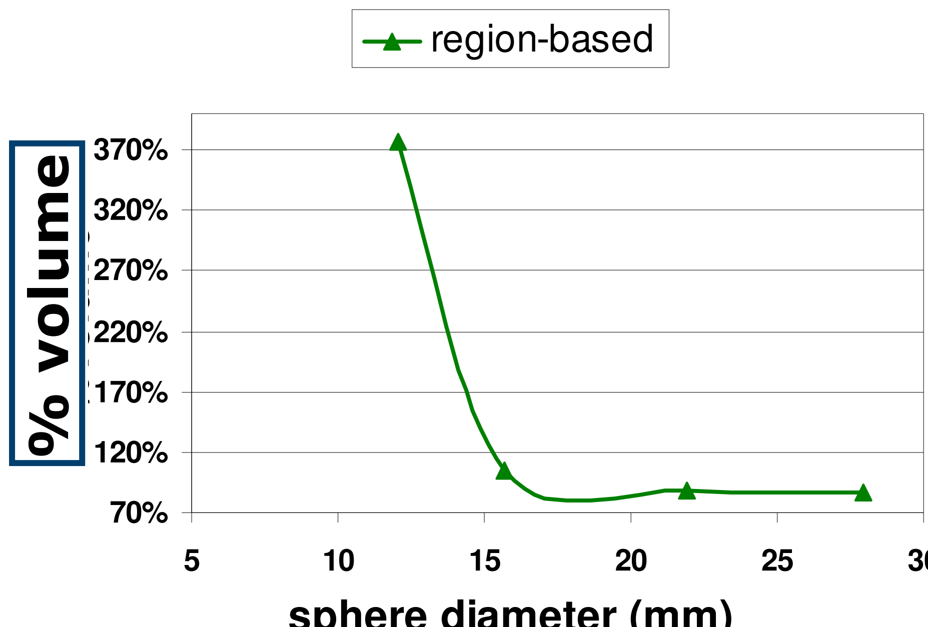

The algorithm (2)

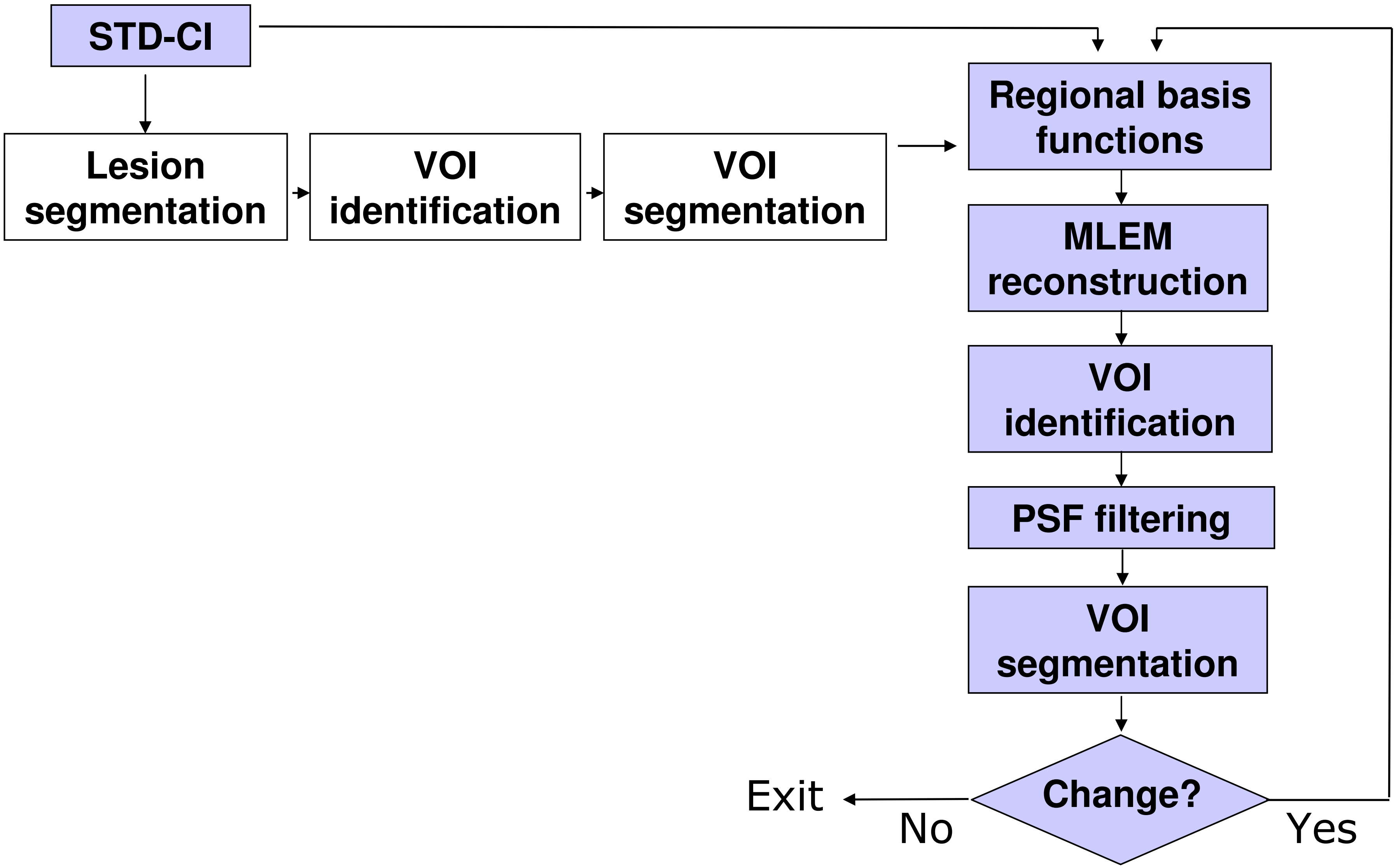

Experimentally scanned sphere phantom: results

Activity contrast=7.5

first iteration last iteration

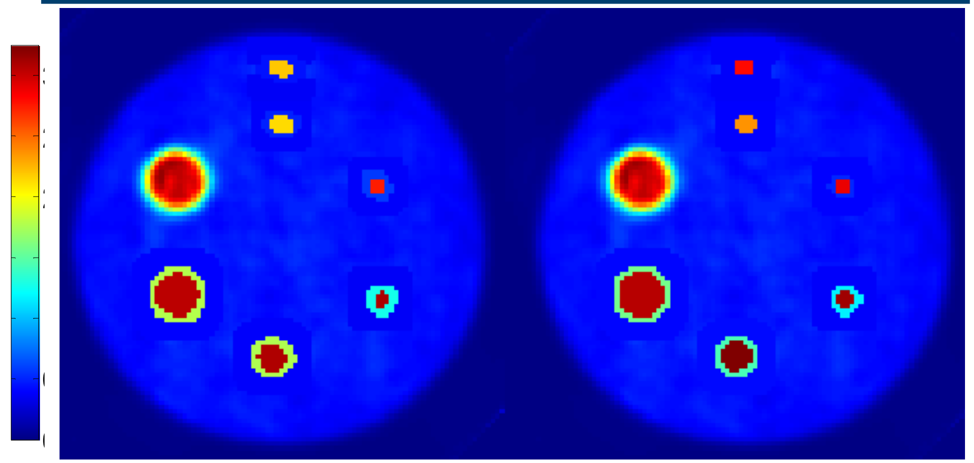

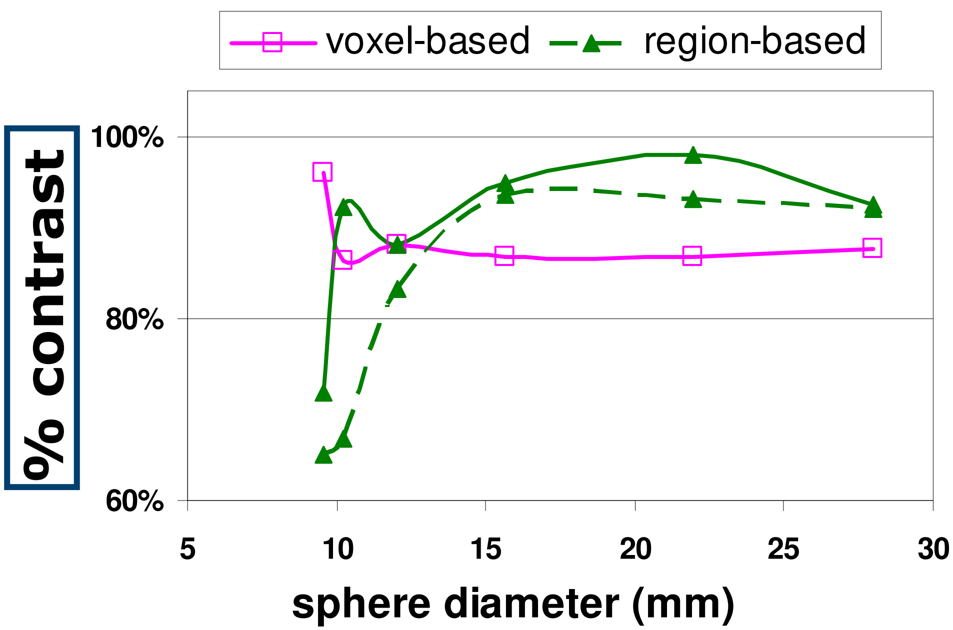

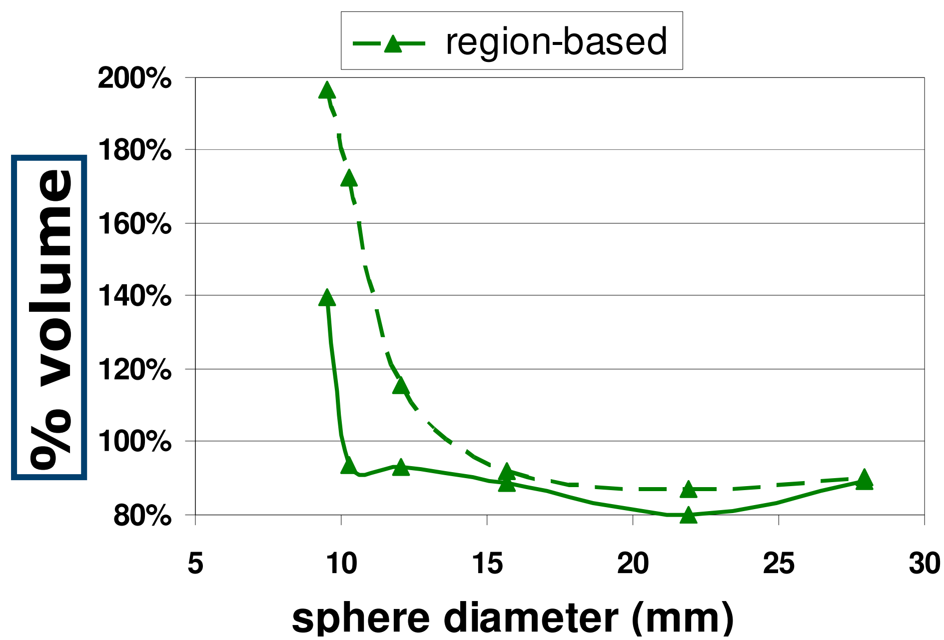

Experimentally scanned sphere phantom: results

Activity contrast=4

first iteration **last iteration**

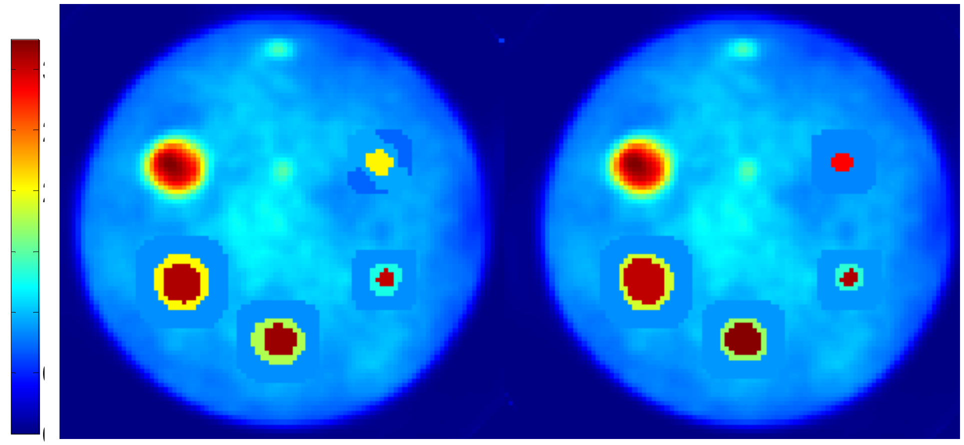

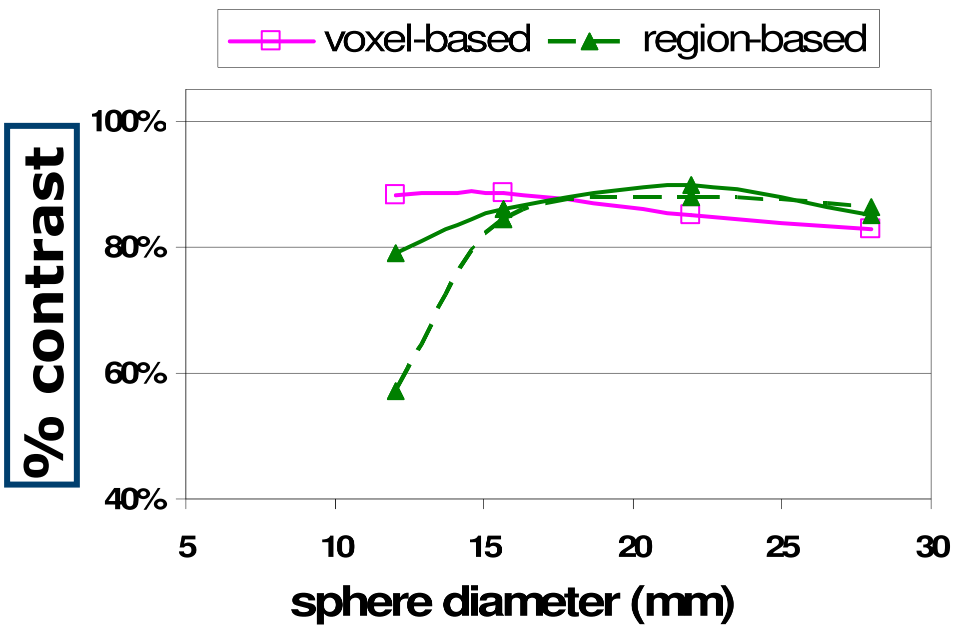

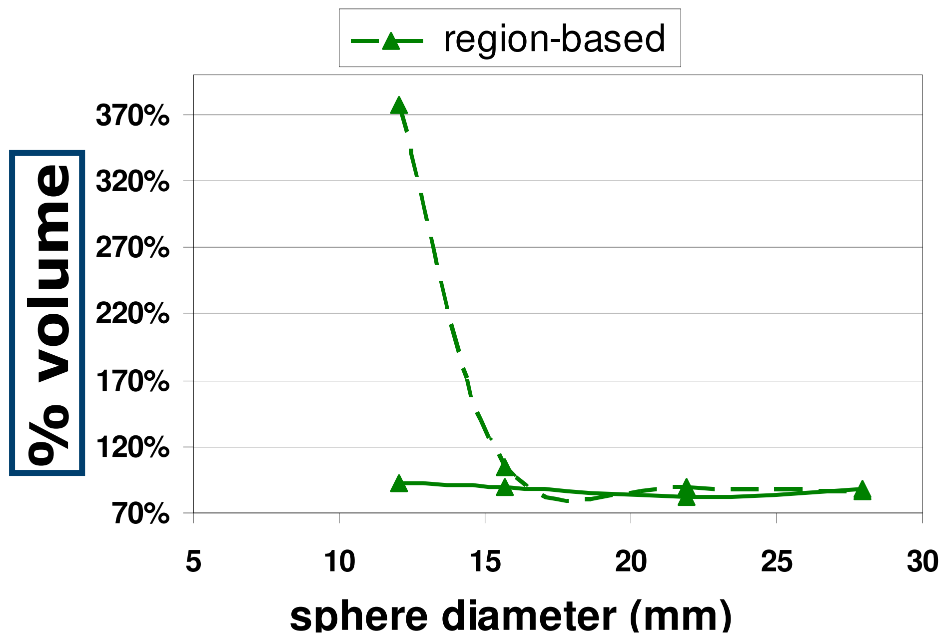

Experimentally acquired sphere phantom: results

Errors in sphere segmentation: robustness evaluation

TBR 7.5

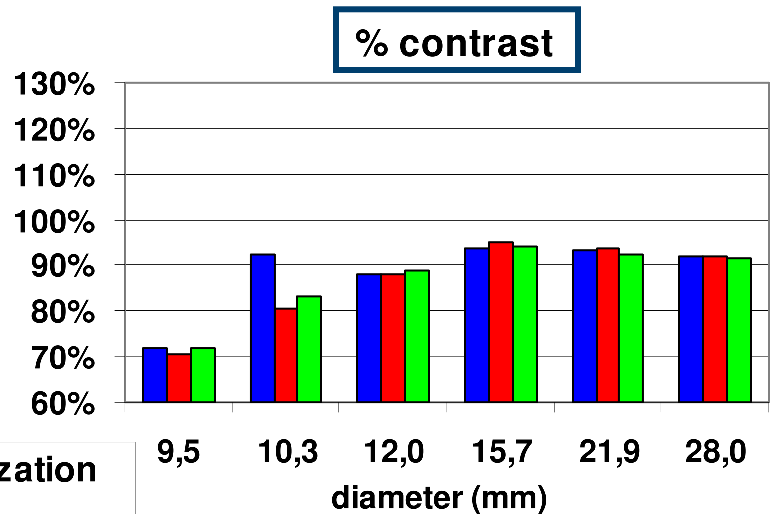

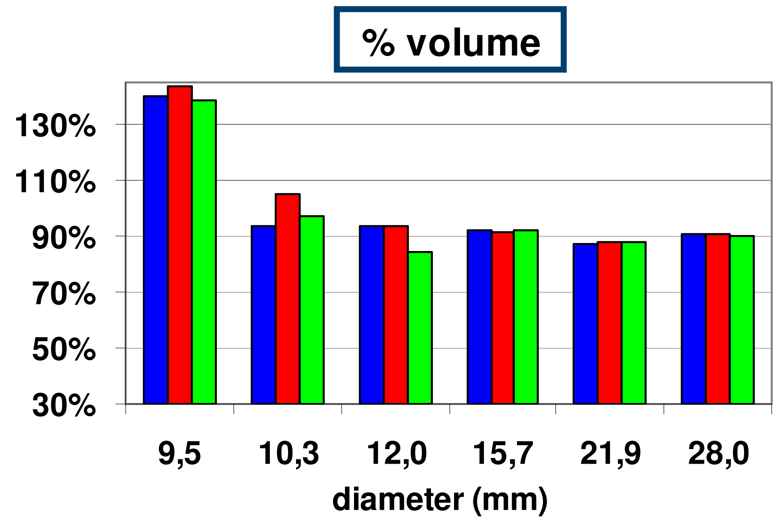

- correct initialization
- error +30%
- error -30%

TBR 4

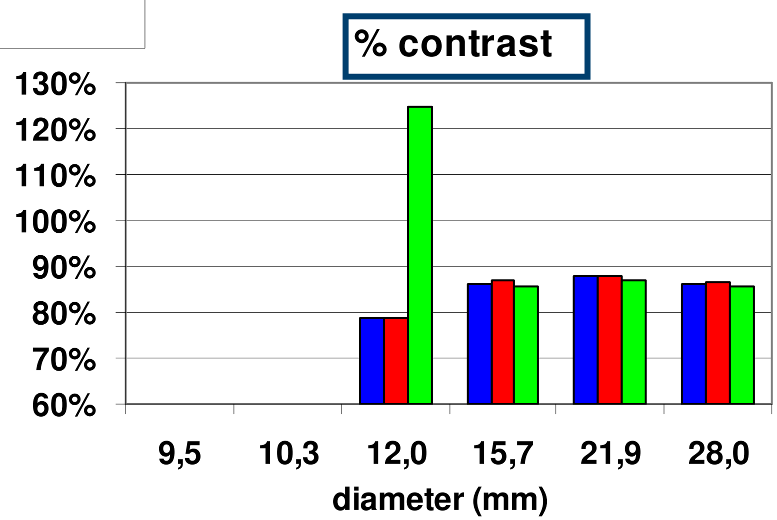

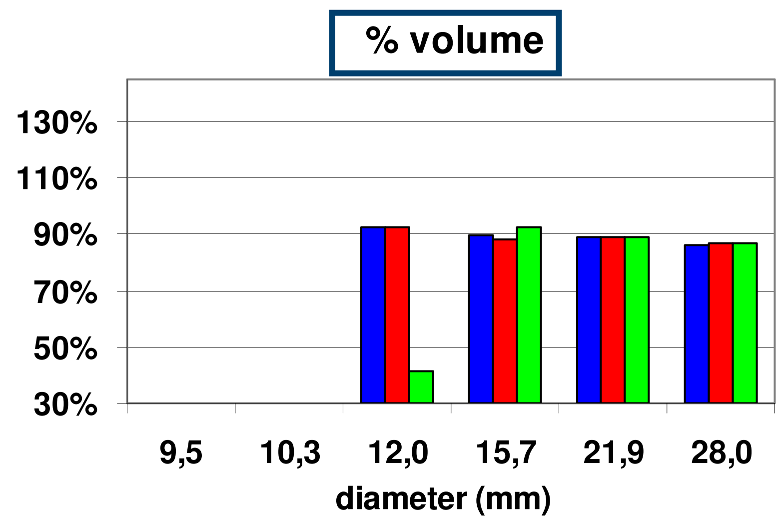

Experimentally acquired sphere phantom: results

TBR 7.5

■ one object segmented ■ all objects segmented

% contrast

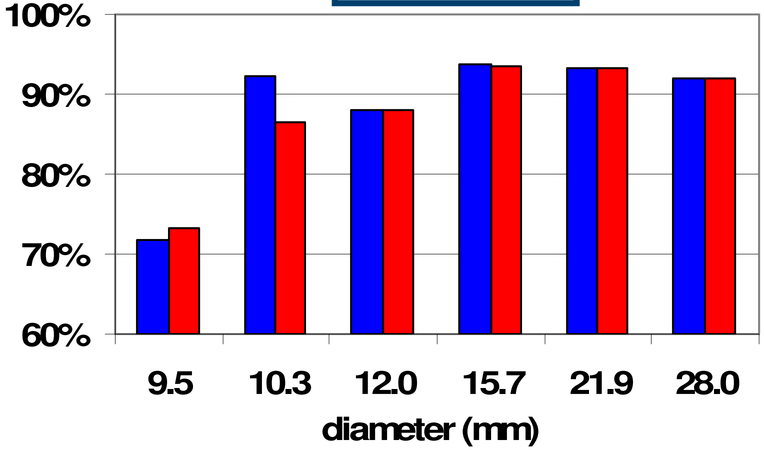

% volume

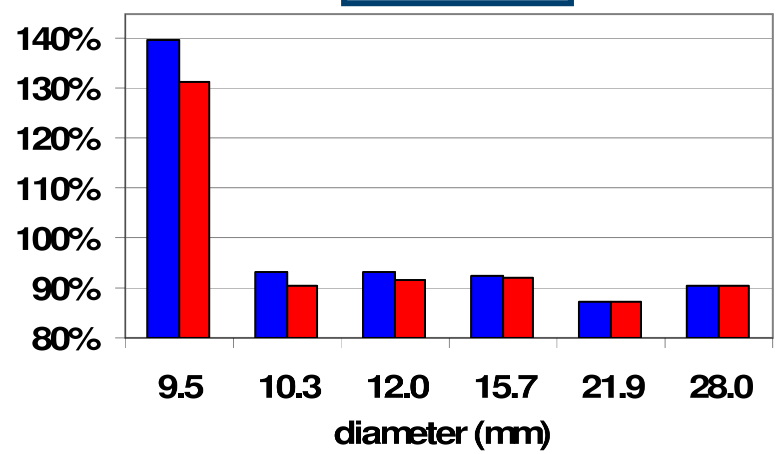

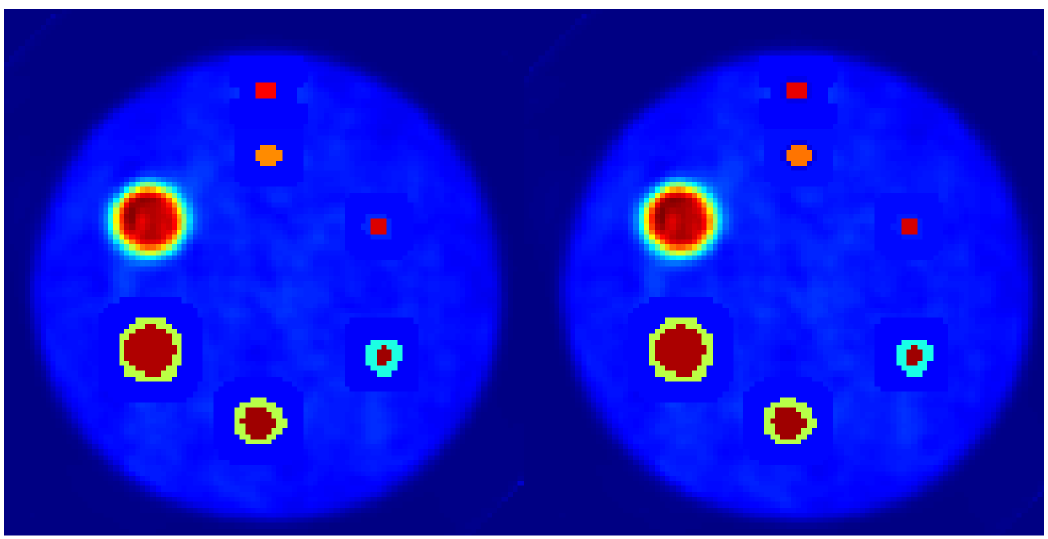

Open problems and brain storming

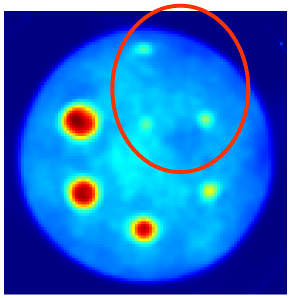

1.Uniform, small, low-contrast objects:

- initial lesion segmentation with acceptable error (±30%)
- VOI segmentation in connected $T_r(x,y,z)$

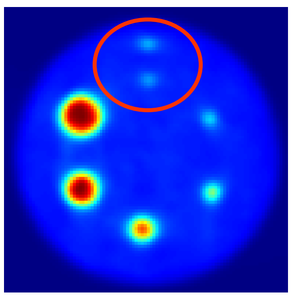

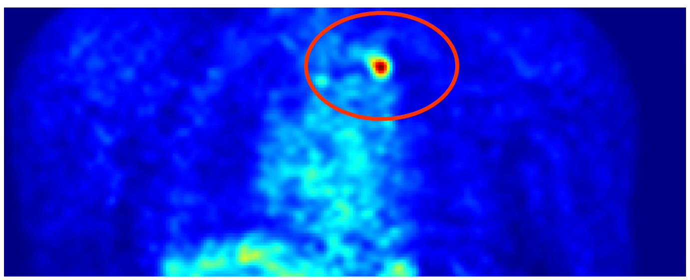

2.Contiguous objects:

- VOI identification
- VOI segmentation in Tr(x,y,z)

3.Inhomogeneous objects:

- VOI segmentation in Tr(x,y,z)